Optimization of the Variable Inertia Rotational Mechanism using Machine Learning

A. T. Sarkar[1] and N. E. Wierschem[1]

[1] The University of Tennessee, Knoxville 37996, TN, USA

Abstract. Rotational inertial mechanisms can produce mass amplification effects with only a small physical mass by converting translation to the rotation of a flywheel, which makes them attractive for structural control applications. A variable inertia rotational mechanism (VIRM) is a nonlinear mechanism in which masses in the flywheel can move radially, causing variable inertia. The performance of the VIRM depends on its parameters and the objectives considered. This paper presents the optimum parameters of the VIRM in a single-degree-of-freedom (SDOF) system using an artificial neural network (ANN) model. Optimum VIRM values of several sets of SDOF systems are used to train the ANN model. These values are determined using numerical simulations, and the RMS amplitude of total energy in the system is considered the optimization objective. Numerical simulations of VIRM systems are presented to demonstrate the effectiveness and examine the ANN-based machine learning optimization process's performance.

Keywords: Variable inertia rotational mechanism, Nonlinear, Optimal damping, Machine learning, Artificial neural network.

1 Introduction

With the development in passive control systems, rotational inertia mechanisms have become popular in civil structures to improve the dynamic response of structures. The linear rotational inertia element, most commonly known as 'inerter', can produce a great deal of effective mass with a relatively small physical mass by transforming translational motion to the rotational motion of a flywheel. The inerter is a two-terminal mechanical element which produces equal and opposite forces proportional to the relative acceleration between the two terminals [1]. Ball–screw, lead-screw, rack and pinion, and hydraulic mechanisms connected to a flywheel have been utilized to realize the inerter [1]–[4].

Inerters have been investigated in combination with tuned-mass-dampers to control structural vibration [5]–[7]. In addition, researchers have utilized inerters together with toggle braces, electromagnetic damper, friction pendulum, and a structure's external rocking wall, to mitigate the dynamic response of structures [8]–[11]. Investigations related to passive control with these devices have mostly considered linear rotational inertia mechanisms (inerters) that generate constant effective mass. Recently, research

has been conducted to understand the dynamics of nonlinear rotational inertia mechanisms that produce variable rotational inertia and thus variable mass effects.

There exist various types of variable rotational inertia mechanisms (VIRM) but the work presented in this paper will consider a varied inertance mechanism resulting from changes in mass distribution of a flywheel related to the flywheel's rotational velocity. The VIRM components include multiple symmetrically spaced mass-spring-dampers placed in a flywheel. The flywheel is connected to the structure using a ball-screw. When the structure is excited, it drives the ball-screw, which results in the rotation of the flywheel. Hence, with the response of the structure, the masses in the flywheel are pushed outward towards the boundary of the flywheel, which causes the variable moment of inertia of the flywheel.

Note that the flywheel angular velocity ($\dot{\theta}$) is proportional to the relative velocity ($\dot{u}$) of the structure between the attachment points of the VIRM and can be expressed as,

$$\dot{\theta} = \alpha \dot{u} \tag{1}$$

where α is $2\pi/\rho$ given a VIRM utilizing a ball-screw and ρ is the lead of the ball-screw.

The performance of VIRMs relies on the selection of optimized parameters, such as the normalized damping factor associated with the masses in the flywheel. Several numerical optimization criteria have been developed to obtain the optimum design parameters. Due to the nonlinear nature of the VIRM, these optimization processes may become time-consuming; therefore, there is interest in utilizing machine learning techniques to aid in optimization efforts

This work studies the used of an artificial neural network (ANN) to produce optimum VIRM parameters. Numerical simulations are performed on a single-degree-of-freedom (SDOF) primary structure with VIRM subjected to different amplitudes of random excitation. An exhaustive search is done on various normalized slider damping factors to determine the structure's total energy. Finally, the ANN model is trained using the dataset from the numerical simulations to aid in determining optimal slider damping.

2 Equation of motion of structure with VIRM

The VIRM flywheel consists of symmetrically placed spring-mass-dampers where the masses can only move in the radial direction. The springs of the VIRM have a trilinear elastic force-displacement relationship with soft stiffness (k_{sd}) in the middle and two stiffer penalty spring (k_p) segments near the center and the edge of the flywheel. The stiff penalty springs restrain the movement of the masses inside the flywheel. The static moment of inertia of the VIRM flywheel assembly is

$$J_T = \frac{1}{12} n m_{sd} \left(\frac{3}{4} v_{sd}^{\ 2} + h_{sd}^{\ 2} \right) + \frac{1}{2} m_c r^2 + n m_{sd} x^2 \tag{2}$$

where n, m_{sd}, v_{sd}, h_{sd}, m_c, r and x are the number of sliders, slider mass, slider diameter, slider height, mass of the flywheel without the sliders, radius of the flywheel and displacement of the slider, respectively. The total moment of inertia of the flywheel includes the static moment of inertia and the inertia generated by the movement of the slider masses in the flywheel.

Fig. 1 depicts the damped SDOF system with mass m_s, stiffness k_s, viscous damping c_s and passive control provided with the VIRM subjected to external force $F(t)$. The non-dimensional equation of motion of the system can be expressed as

$$U'' + \left(\frac{1}{12} n \mu_1 \left(\frac{3}{4} v_{sd}^{\ 2} + h_{sd}^{\ 2} \right) + \frac{1}{2} \mu_2 r^2 \right) \alpha^2 U'' + 2 n \mu_1 \alpha^2 \beta X X' U' + n \mu_1 X^2 \alpha^2 U'' + 2 \xi_s U' + U = F(t)$$
$$X'' - X \frac{\alpha^2}{\beta} U'^2 + F_B + 2 D_{sd} X' = 0 \tag{3}$$

where, F_B represents the restoring force of the trilinear springs, which depends on the radial position of the slider masses and can be defined as

$$\begin{aligned} F_B &= R_{\min} - x_0 + \kappa (X - R_{\min}),\ X < R_{\min} \\ F_B &= X - x_0,\ R_{\min} \le X < R_{\max} \\ F_B &= = R_{\max} - x_0 + \kappa (X - R_{\max}),\ X \ge R_{\max} \end{aligned} \tag{4}$$

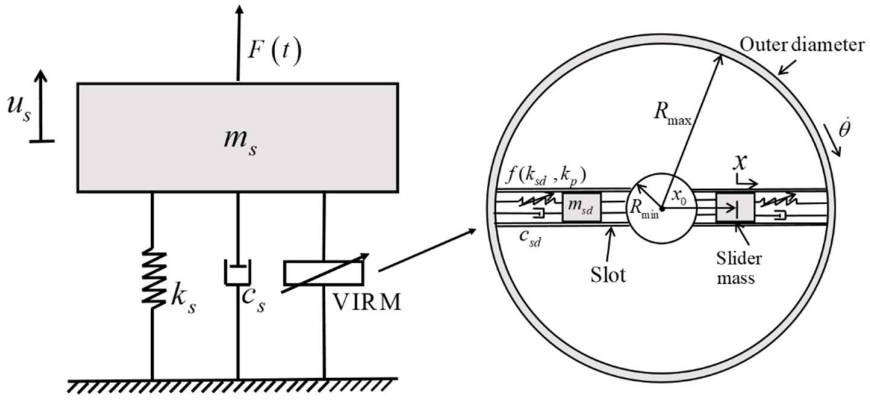

Fig. 1. Schematic representation of a SDOF structure with a VIRM (left), diagram of the VIRM flywheel with two slider masses located at their initial position (right)

The parameters of the system and their associated values used for this study are as follows,

$\mu_1 = \frac{m_{sd}}{m_s} = 0.0005$: slider mass ratio; $\mu_2 = \frac{m_c}{m_s} = 0.0017$: flywheel mass ratio without slider masses;

$\beta = \frac{\omega_{sd}}{\omega_{s_0}} = 14.64$: frequency ratio; $\kappa = \frac{k_p}{k_{sd}} = 100$: stiffness ratio;

$\xi_s = \frac{c_s}{2m_s\omega_{s_0}} = 0.02$: main structure damping ratio; $\alpha = 100$: relationship between $\dot{\theta}$ and $\dot{u}$;

$\omega_{s_0} = \sqrt{\frac{k_s}{m_s}} = 2.91$ Hz: natural frequency of the main structure without VIRM/FIRM;

$\omega_{sd} = \sqrt{\frac{k_{sd}}{m_{sd}}} = 42$ Hz: natural frequency of the the slider mass;

$D_{sd} = \frac{c_{sd}}{2m_{sd}\omega_{sd}}$: normalized damping factor of the slider mass; $F(t) = \frac{P(t)}{k_s}$: normalized force amplitude;

$U = u$: displacement of the main structure; $U' = \frac{\dot{u}}{\omega_{s_0}}$: normalized velocity of the main structure;

$U'' = \frac{\ddot{u}}{\omega_{s_0}^2}$: normalized acceleration of the main structure; $X = x$: displacement of the slider;

$X' = \frac{\dot{x}}{\omega_{sd}}$: normalized velocity of the slider; $X'' = \frac{\ddot{x}}{\omega_{sd}^2}$: normalized acceleration of the slider;

$v_{sd} = 0.02$ m : slider diameter; $h_{sd} = 0.02$ m: slider height; $r = 0.1$m: radius of the flywheel;

$x_0 = 0.01$m : initial position of the slider; $R_{\max} = 0.095$m : radial position of the upper penalty spring;

$R_{\min} = 0.005$m : radial position of the lower penalty spring;

3 VIRM optimization

The optimum D_{sd} of the VIRM, the normalized damping factor of the slider, is determined using the exhaustive search technique. In this study, the response of the SDOF structure with the VIRM (four slider masses) with different D_{sd} is simulated under different RMS white noise levels using the MATLAB implicit solver. The RMS of the total energy in the response is measured. The VIRM D_{sd} that produces the minimum RMS total energy is considered the optimum D_{sd}. The optimum D_{sd} for each noise level is determined from the minimum of the curve fitted from the RMS energy versus D_{sd} data.

Fig. 2 presents the RMS energy of the SDOF structure for different slider damping levels under two white noise amplitudes. This figure shows the numerical simulation results and the fitted curve of the results. It can be observed that the RMS energy decreases as the D_{sd} increases and the RMS total energy reaches a minimum when D_{sd} is 1283 for the normalized RMS noise amplitude of 0.21. This D_{sd} is considered the optimum normalized slider damping factor. Afterward, the RMS energy increases as higher slider damping is added. A similar trend is noticed for a higher RMS noise; the RMS energy decreases until it reaches a D_{sd} of 3778. Note that D_{sd} is not similar to the general linear damping ratio as the VIRM is nonlinear. The impact of the slider damping level

will change depending on the system response because of dependencies in the system EOM related to the radial position of the slider masses and the relative velocity of the primary structure.

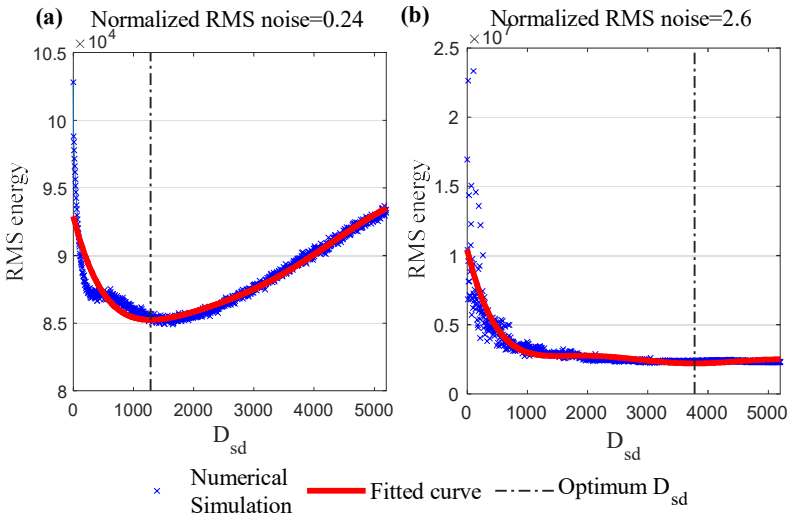

Fig. 2. RMS energy for different D_{sd} for different white noise: (a) Normalized RMS noise =0.21, (b) Normalized RMS noise=2.66

4 Artificial neural network

An artificial neural network is a parallel computational model based on simulated human brain functionality. In this study, a feed-forward neural network is applied. A feed –forward neural network consists of an input layer, where the inputs of the problem are received, hidden layer, which adjusts the weights to determine the relationship between inputs and outputs, and an output layer which produces outputs (**Fig. 3**). The inputs to the model are the RMS amplitude of white noise and $D_{sd,}$ and the output is the RMS value of the total energy. The network used in the study is trained using 30 neurons in the hidden layer. The MATLAB neural network fitting wizard app is utilized, and the 'Lavenberg-Marquardt' training algorithm is selected to develop a nonlinear relationship between inputs and targets using the available dataset. The data is randomly selected for three subsets: 70% for training, 15% for validation, and 15% for testing. The validation dataset is used to halt the learning algorithm when the generalization starts improving. The testing dataset shows an independent measure of how the network performs after training.

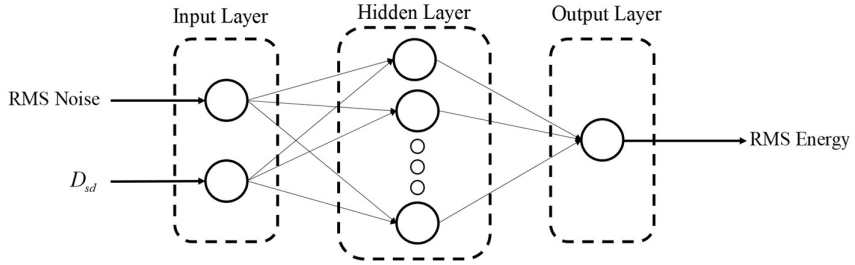

Fig. 3. Schematic diagram of ANN model

5 Estimation and prediction of VIRM damping ratio

To investigate the dynamic effect of the VIRM, the structure is excited with 20 different white noise levels for a range of D_{sd}. The normalized RMS amplitude of the white noise ranges from 0.24 to 5.32, with an incremental difference of 0.26. The training is done for the VIRM D_{sd} ranging from 0 to 6000 with an increment of 4 for each RMS noise. All structures analyzed have 2% inherent damping in the primary structure. The generated ANN model is utilized to find the RMS total energy results for D_{sd}. **Fig. 4** compares the RMS total energy from the ANN model and numerical simulation. The figure shows similar RMS energy characteristics in response to the VIRM D_{sd} for both the simulation results and as predicted by the ANN.

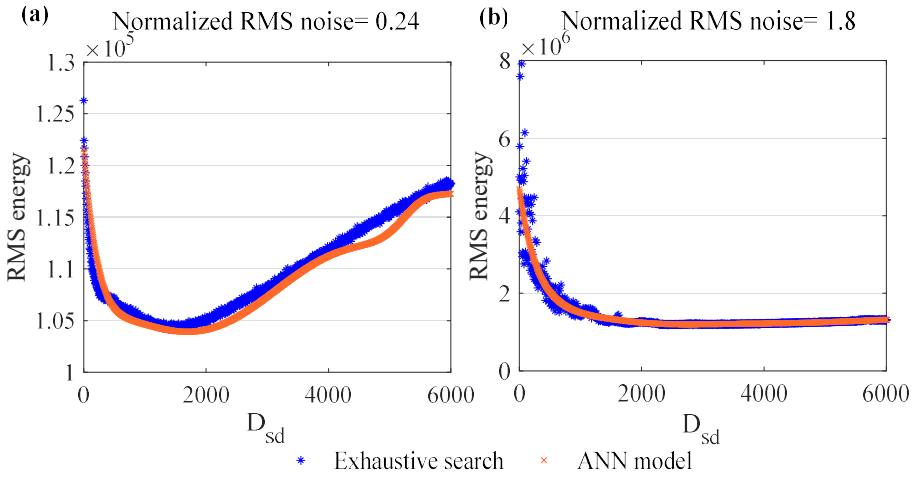

Fig. 4. Comparison of predicted and simulated RMS total energy for D_{sd} at normalized RMS noise amplitude: (a) 0.24 (b) 1.8

Higher-order polynomial curve fitting technique is applied to the output results. The D_{sd} that produces the minimum RMS energy in the curve fitted data is considered the

sliders' optimum D_{sd}. **Fig. 5** presents the D_{sd} resulting from the ANN predicted model and the exhaustive search. It can be observed that the predicted results from the ANN model are close to the optimum obtained from the exhaustive search method. The maximum difference between the normalized damping factor is 10.88% when the normalized RMS noise amplitude is 0.59. Additionally, the average difference between the predicted and simulated results is 2.06%.

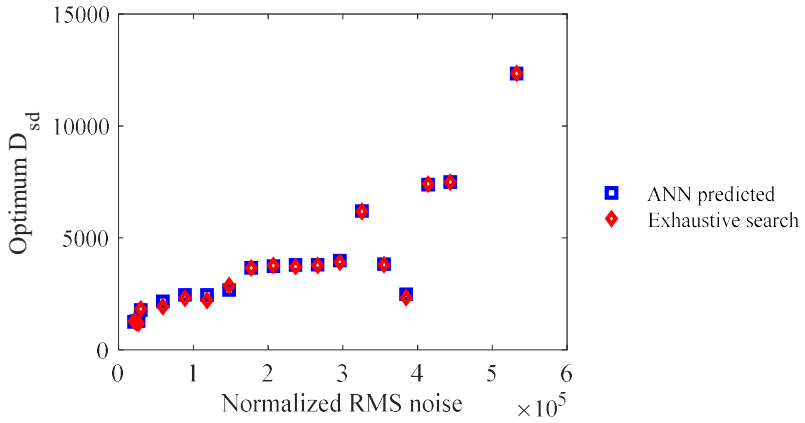

Fig. 5. Comparison of the exhaustive search and the ANN predicted optimum D_{sd} for a range of normalized RMS noise amplitude

6 Conclusion and future study

This paper aims to generate an ANN model to estimate the optimum normalized damping factor of the VIRM in a SDOF system. Through numerical analysis of the SDOF system, a dataset was generated for a range of normalized damping factors of the VIRM and this dataset was utilized to train the model. This proposed model can effectively reduce the computational costs associated with the long iterations in the exhaustive search method and help predict the structure's dynamic response. Although the predicted results are not precise in some cases, the results can be improved by modifying the hidden layer configuration or utilizing a more precise optimization technique to get the training dataset. The results of this work show that once the ANN model is built, it can be an effective tool for finding the optimum VIRM D_{sd} without doing an iterative optimization technique.

7 Acknowledgments

This material is based upon work supported by the National Science Foundation under Grant No. 1944513. Any opinions, findings, and conclusions or recommendations expressed in this material are those of the authors and do not necessarily reflect the views of the National Science Foundation.

References

[1] M. C. Smith, "Synthesis of mechanical networks: the inerter," *IEEE Trans. Autom. Control*, vol. 47, no. 10, pp. 1648–1662, Oct. 2002, doi: 10.1109/TAC.2002.803532.

[2] M. C. Smith, "FORCE-CONTROLLING MECHANICAL DEVICE," US 7,316, 303 B2, Jan. 08, 2008

[3] M. C. Smith, "Force-Controlling Hydraulic Device," US 2021/0199428 A1, Aug. 09, 2012

[4] S. J. Swift, M. C. Smith, A. R. Glover, C. Papageorgiou, B. Gartner, and N. E. Houghton, "Design and modelling of a fluid inerter," *Int. J. Control*, vol. 86, no. 11, pp. 2035–2051, Nov. 2013, doi: 10.1080/00207179.2013.842263.

[5] Y. Hu and M. Z. Q. Chen, "Performance evaluation for inerter-based dynamic vibration absorbers," *Int. J. Mech. Sci.*, vol. 99, pp. 297–307, Aug. 2015, doi: 10.1016/j.ijmecsci.2015.06.003.

[6] A. Javidialesaadi and N. E. Wierschem, "Optimal design of rotational inertial double tuned mass dampers under random excitation," *Eng. Struct.*, vol. 165, pp. 412–421, Jun. 2018, doi: 10.1016/j.engstruct.2018.03.033.

[7] A. Javidialesaadi and N. E. Wierschem, "Energy transfer and passive control of single-degree-of-freedom structures using a one-directional rotational inertia viscous damper," *Eng. Struct.*, vol. 196, p. 109339, Oct. 2019, doi: 10.1016/j.engstruct.2019.109339.

[8] A. Di Egidio, S. Pagliaro, and C. Fabrizio, "Combined Use of Rocking Walls and Inerters to Improve the Seismic Response of Frame Structures," *J. Eng. Mech.*, vol. 147, no. 5, p. 04021016, May 2021, doi: 10.1061/(ASCE)EM.1943-7889.0001920.

[9] J.-S. Hwang, J. Kim, and Y.-M. Kim, "Rotational inertia dampers with toggle bracing for vibration control of a building structure," *Eng. Struct.*, vol. 29, no. 6, pp. 1201–1208, Jun. 2007, doi: 10.1016/j.engstruct.2006.08.005.

[10] Y. Nakamura *et al.*, "Seismic response control using electromagnetic inertial mass dampers: Seismic response control using EIMD," *Earthq. Eng. Struct. Dyn.*, vol. 43, no. 4, pp. 507–527, Apr. 2014, doi: 10.1002/eqe.2355.

[11] Z. Zhao, R. Zhang, Y. Jiang, and C. Pan, "Seismic response mitigation of structures with a friction pendulum inerter system," *Eng. Struct.*, vol. 193, pp. 110–120, Aug. 2019, doi: 10.1016/j.engstruct.2019.05.024.